# Fig. S1 Yanagisawa *et al.*

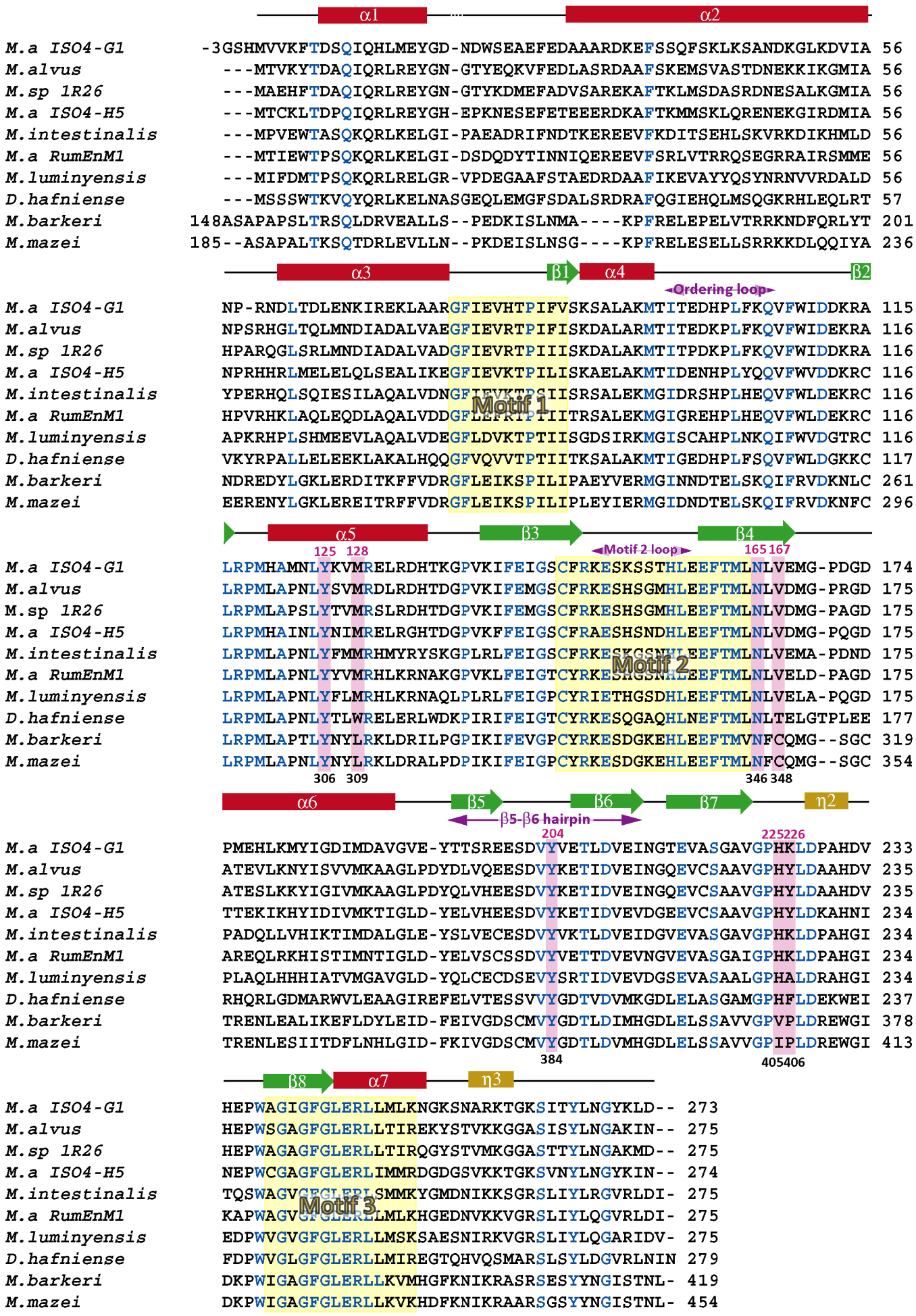

**Fig. S1. Structure-based sequence alignments of ISO4-G1 PylRS and other PylRSs.** The PylRS sequences were aligned with the program CLUSTAL W [77], and then parts of the alignments were adjusted manually. Highly conserved residues among the PylRSs are shown in blue. The secondary structures (α-helices, $3_{10}$ helices, and β-sheets) are shown as wine red bars, olive bars, and green arrows, respectively, above the sequence alignments. Numbers at the top and bottom correspond to the amino acid residues of ISO4-G1 PylRS and *Mm*PylRS, respectively. Dashes represent breaks in the actual amino acid sequences to allow sequence alignments with PylRSs. Motifs 1, 2, and 3 are colored yellow. The ordering loop, the motif-2 loop, and the β5-β6 hairpin are shown on the top line. Amino acid residues that were mutated in this study are colored pink. Accession numbers are as follows. ISO4-G1 PylRS (*M.a* ISO4-G1, AMK13702); *Ma*PylRS (*M. alvus*, WP_015505008); 1R26PylRS (*M. sp 1R26*, WP_058747239); ISO4-H5 PylRS (*M.a* ISO4-H5, WP_066075773); RumPylRS (*M.a RumEnM1*, KQM11560); *Ml*PylRS (*M. luminyensis*, WP_019176308); *Mt*PylRS (*M. termitum*, WP_048111907); *Mi*PylRS (*M. intestinalis*, WP_020448777); *Dh*PylSc (*D. hafniense*, WP_018307530); *Mb*PylRS (*M. barkeri*, Q6WRH6); and *Mm*PylRS (*M. mazei*, Q8PWY1).

**Fig. S2 Yanagisawa *et al.***

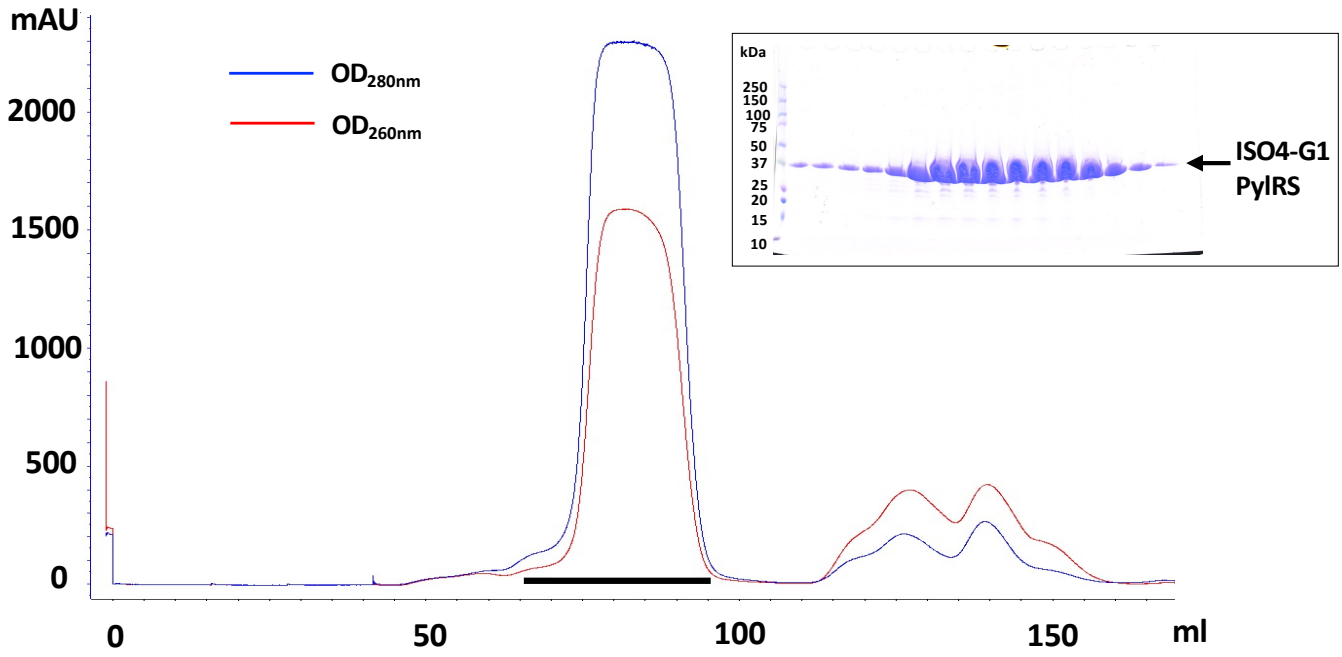

**Fig. S2. Chromatogram for the purification of ISO4-G1 PylRS by Superdex 200 size-exclusion chromatography.** SDS-PAGE analysis of the ISO4-G1 PylRS fractions (inset). The absorbances of the ISO4-G1 PylRS fractions are saturated at 280 nm and 260 nm. The black bar represents the range of fractions subjected to SDS-PAGE analysis.

# Fig.S3 Yanagisawa *et al.*

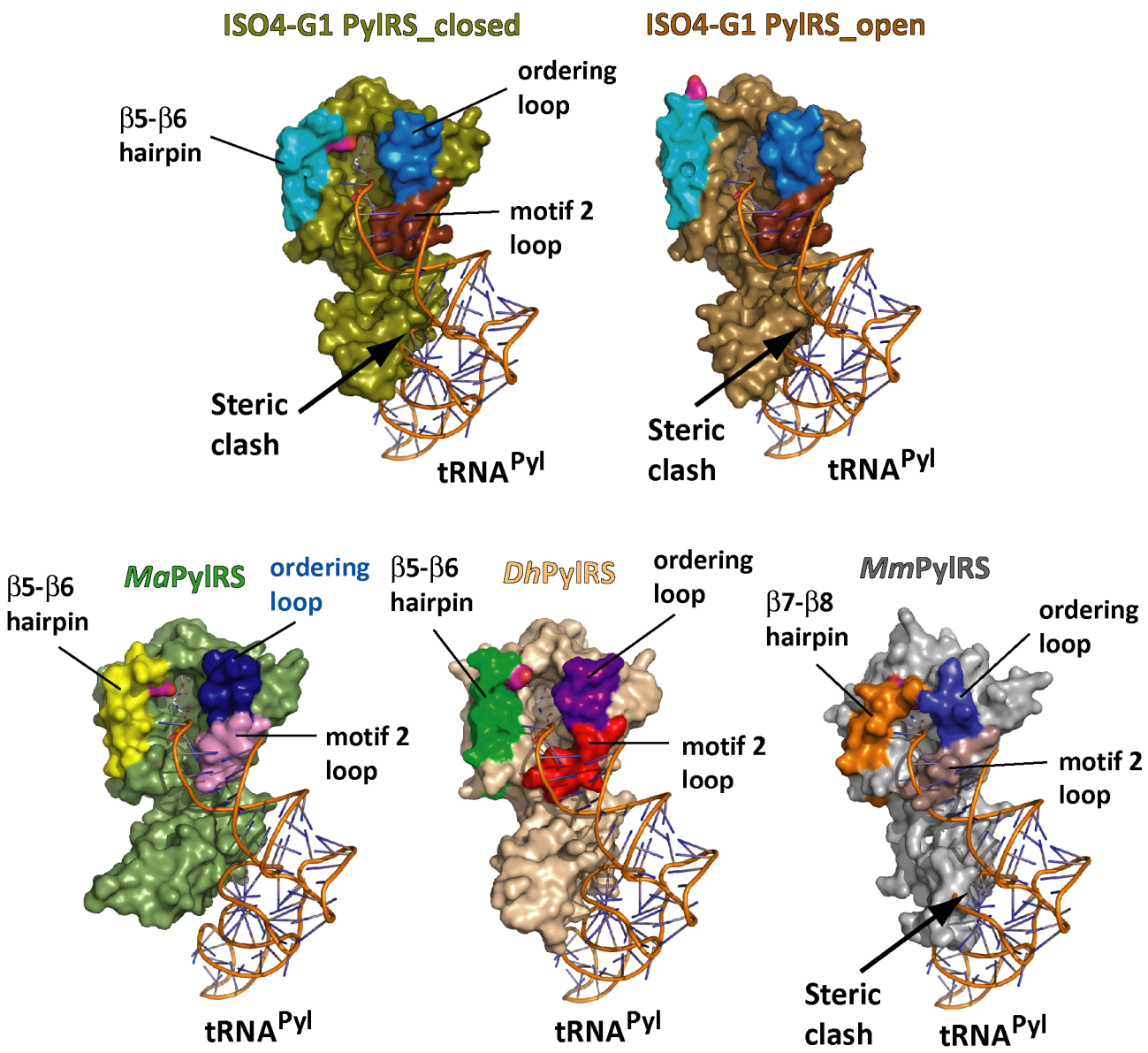

**Fig. S3. Structural comparison of ISO4-G1 PylRS with *Ma*PylRS, *Mm*PylRSc, and *Dh*PylSc•tRNA$^{Pyl}$.**

Superimpositions of the ISO4-G1 PylRS with the *Ma*PylRS, the *Dh*PylSc•tRNA$^{Pyl}$ complex (PDB code: 2ZNI), the apo form (PDB: 2E3C), and the Pyl-AMP-bound *Mm*PylRSc (PDB: 2ZIM) structures, represented by surface models. The ordering loop, the motif-2 loop, and the β5-β6 hairpin (β7-β8 hairpin in *Mm*PylRS) are colored differently. The catalytic core structures of ISO4-G1 PylRS, *Ma*PylRS, *Dh*PylSc, and *Mm*PylRSc superimposed well, but the two α-helices (α1 and α2) of *Mm*PylRSc are slightly tilted and cause steric hindrance with tRNA$^{Pyl}$.

**Fig. S4 Yanagisawa *et al.***

**a** **Open (molecule A)**

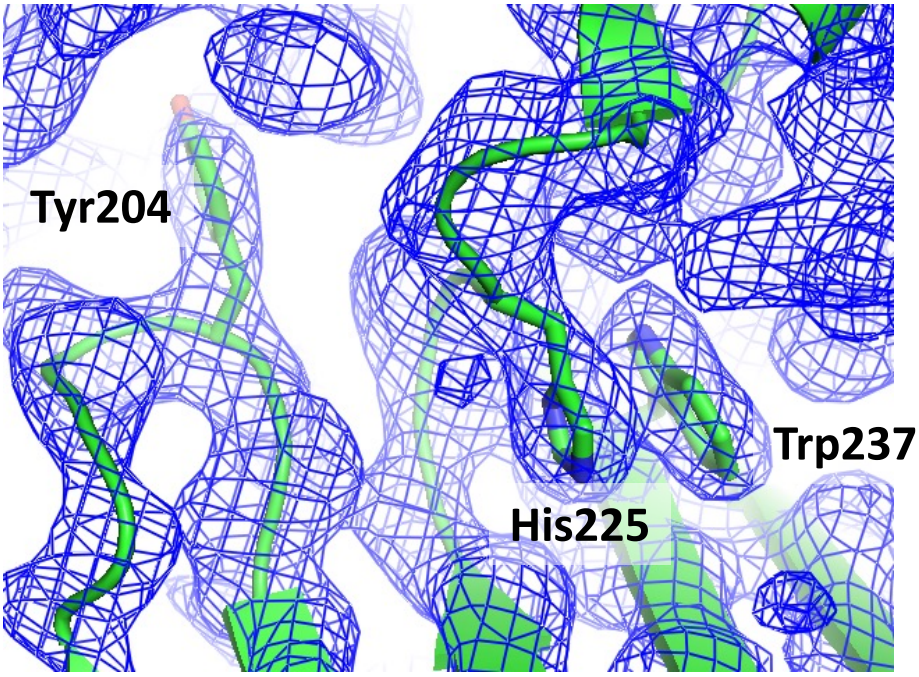


**b** **Closed (molecule B)**

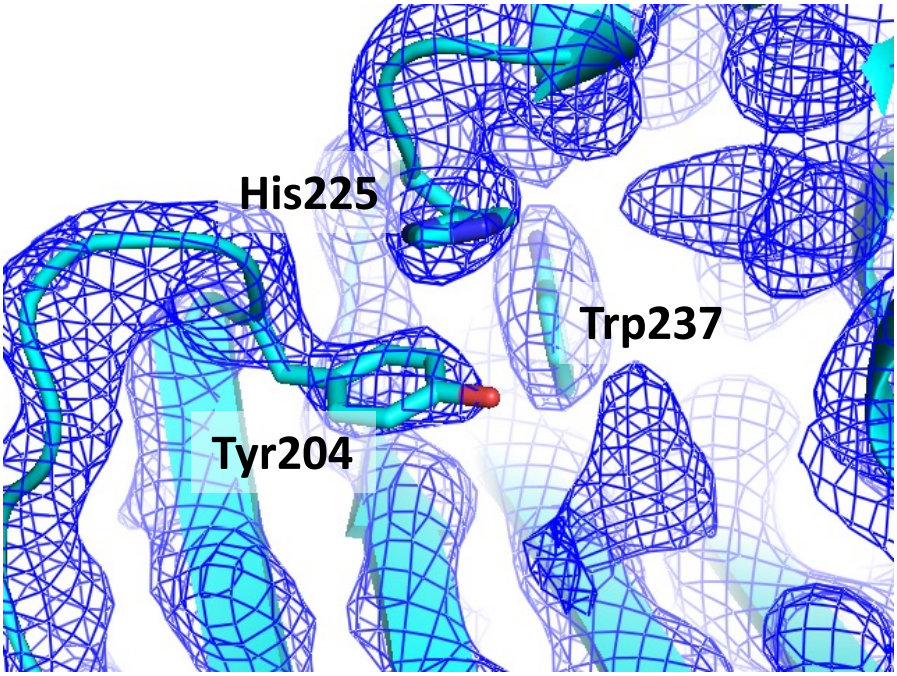

**Fig. S4. Electron density map of the β5-β6 region in the ISO4-G1 PylRS structure.** The 2*Fo-Fc* electron density map for the regions around Tyr204, His225, and Trp237 is represented as a blue mesh at a contour level of 1σ. (a) The open conformation. (b) The closed conformation. The Tyr204, His225, and Trp237 residues are shown as stick models.

Fig. S5 Yanagisawa *et al*.

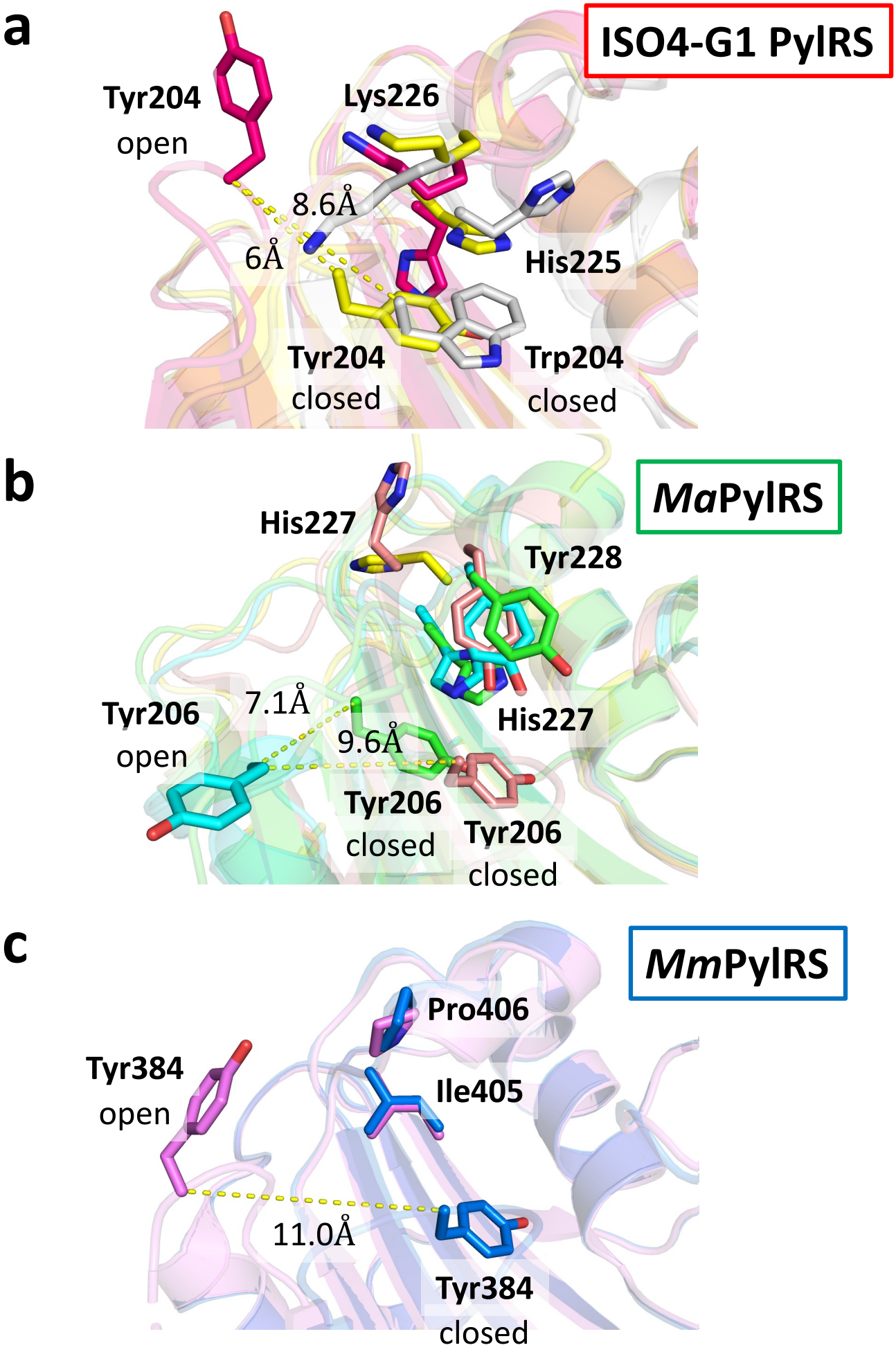

**Fig. S5. Conformational changes of the active-site residues in the open and closed forms of the ISO4-G1 PylRS, *Ma*PylRS, and *Mm*PylRS structures.** (a) The open and closed conformations of the ISO4-G1 PylRS apo form (magenta and yellow, respectively), and the closed conformation of the ISO4-G1 PylRS mutant (7R6O, white). (b) The open and closed conformations of the *Ma*PylRS apo form (6JP2, cyan and light green, respectively), and the closed conformation of the *de novo* screened *Ma*PylRS(N166A/C168G/W239C) mutant bound to acrydonylalanine and AMPPNP (8DQG, vermilion). Tyr206 is disordered in the AMPPNP-bound form (8DQG, yellow). (c) The open conformation of the *Mm*PylRS apo form (pink), and the closed conformation of *Mm*PylRS bound to pyrrolysyladenylate (2Q7H, sky blue). The translucent ribbon models are shown in the background. The ISO4-G1 PylRS Tyr205 residue corresponds to Tyr206 in *Ma*PylRS, and to Tyr384 in *Mm*PylRS. The ISO4-G1 PylRS His225 residue corresponds to His227 in *Ma*PylRS, and to Ile405 in *Mm*PylRS.The ISO4-G1 PylRS Lys226 residue corresponds to Tyr228 in *Ma*PylRS, and to Pro406 in *Mm*PylRS. Each residue is shown as a stick model.

# Fig.S6 Yanagisawa *et al.*

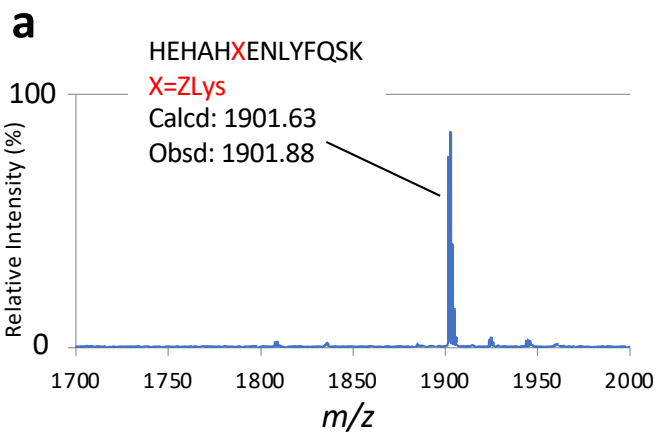


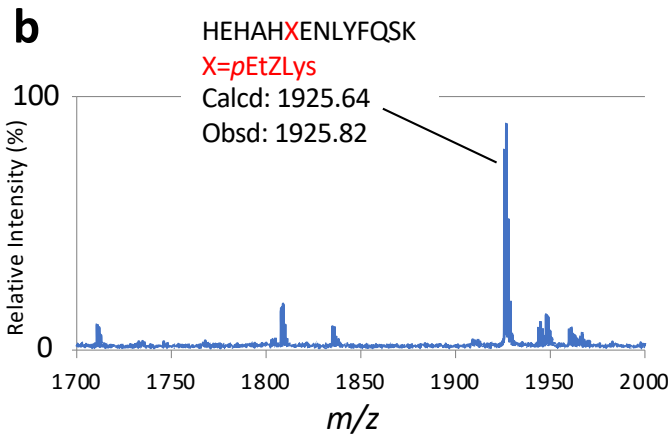


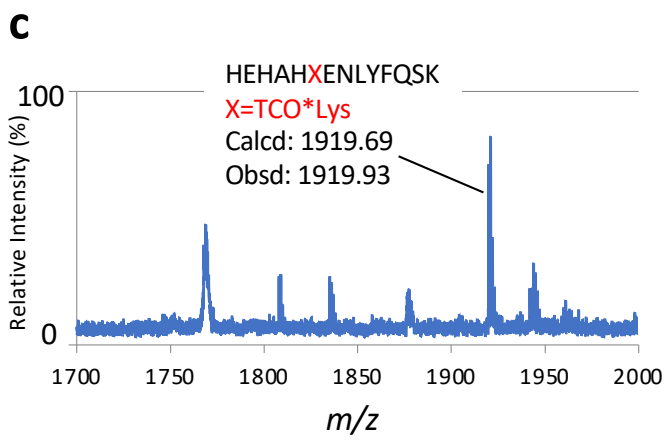


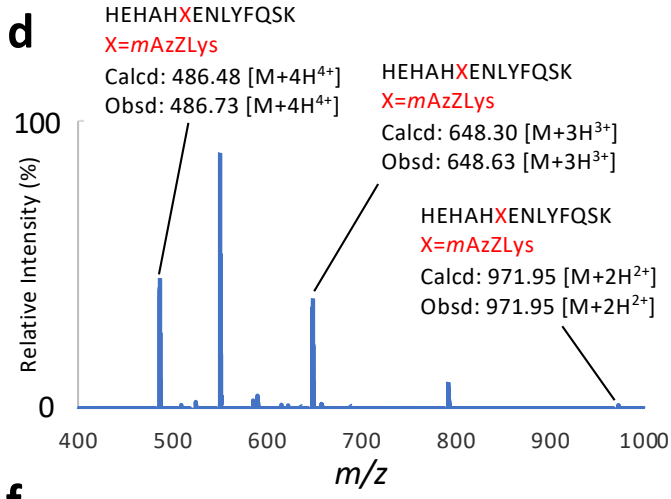


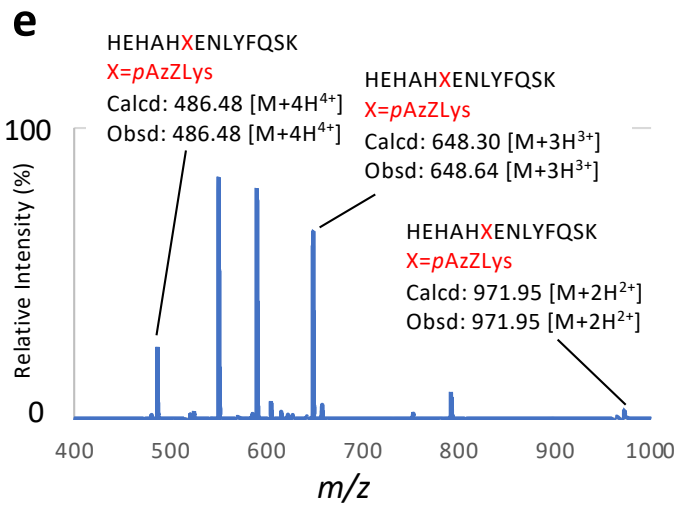


**f**

N11-17amber-GFPS1 sequence

MKDHLIHNHHKHEHAHXENLYFQSKGEELFTGVVPIL
VELDGDVNGHKFSVSGEGEGDATYGKLTLKFICTTGK
LPVPWPTLVTTLTYGVQCFSRYPDHMKRHDFFKSAM
PEGYVQERTISFKDDGNYKTRAEVKFEGDTLVNRIELK
GIDFKEDGNILGHKLEYNYNSHNVYITADKQKNGIKA
NFKIRHNIEDGSVQLADHYQQNTPIGDGPVLLPDNH
YLSTQSALSKDPNEKRDHMVLLEFVTAAGITHGMDE
LYK

**Fig. S6. Mass spectrometry analysis of N11-GFPS1 proteins containing non-canonical amino acids.** The amino acid sequence of GFPS1, with a 24-residue N11-peptide tag at the N-terminus, is shown in (f). The codon of the N11-GFPS1 residue Ala17, which is highlighted by a red X, is mutated to an amber (UAG) codon. The incorporations of ZLys (a), *p*EtZLys (b), and TCO*Lys (c), at position 17 in N11-GFPS1, were confirmed by MALDI-TOF analyses. The incorporations of *m*AzZLys (d) and *p*AzZLys (e), at position 17 in N11-GFPS1, were confirmed by ESI-MS analyses of the tryptic peptide HEHAHXENLYFQSK (X represents a non-canonical amino acid). The observed molecular masses agreed well with the calculated masses.

## Table S1

Data collection and refinement statistics.

| | ISO4-G1 PylRS |
|---|---|
| PDB code | 8IFJ |
| X-ray source | SPring-8<br>BL32XU |
| No. of crystals | 1 |
| Wavelength | 1.0000 |
| Space group | $P2_12_12_1$ |
| Cell dimensions | |
| *a* (Å) | 98.51 |
| *b* (Å) | 102.68 |
| *c* (Å) | 349.86 |
| α, β, γ (°) | 90, 90, 90 |
| Resolution (Å) | 50–2.78 (2.85–2.78) |
| I/σ (I) | 14.47 (1.32) |
| Completeness (%) | 99.73 (99.77) |
| No. reflections | 90,164 |
| Redundancy (%) | 5.99 (6.07) |
| [a]$R_{meas}$ | 0.16 (1.94) |
| Refinement | |
| [b]$R_{work}$ / [c]$R_{free}$ (%) | 23.3/29.5 |
| Resolution (Å) | 49.9–2.78 |
| No. atoms | |
| protein | 21,566 |
| water | 49 |
| No. reflections | |
| (total / test) | 90,021/1,999 |
| Average B-factors | |
| protein | 100.10 |
| water | 57.18 |
| R.m.s. deviations | |
| Bond length (Å) | 0.004 |
| Bond angles (°) | 0.640 |
| Ramachandran plot | |
| Most favored (%) | 96.09 |
| Allowed (%) | 3.91 |
| Disallowed (%) | 0.00 |

The numbers in parentheses are for the last shell.

[a] $R_{meas} = S_{hkl}(n^{1/2}/(n\text{-}1)^{1/2})S_i |I_{avg}\text{-}I_i| / S_{hkl} S I_i$.

[b] $R_{work} = S_{hkl} |F_o\text{-}F_c| / S_{hkl} F_o$ for reflections of work set.

[c] $R_{free} = S_{hkl} |F_o\text{-}F_c| / S_{hkl} F_o$ for reflections of test set [2.2% of total reflections for ISO4-G1 PylRS].